Differential Nanotoxicological and Neuroinflammatory Liabilities of Non-Viral Vectors for RNA Interference in the Central Nervous System

Bruno M. D. C. Godinho[1,2], *David J. McCarthy*[1,2], *Cristina Torres-Fuentes*[3], *Caroll J. Beltrán*[4,5], *Joanna McCarthy*[1], *Aoife Quinlan*[1], *Julien R. Ogier*[6], *Raphael Darcy*[6], *Caitriona M. O'Driscoll*[1], *John F. Cryan*[2,4*]

[1]Pharmacodelivery group, School of Pharmacy, University College Cork, Cork, Ireland

[2]Dept. Anatomy and Neuroscience, University College Cork, Cork, Ireland

[3]Food for Health Ireland, University College Cork, Cork, Ireland

[4]Laboratory of Neurogastroenterology, Alimentary Pharmabiotic Centre, Cork, Ireland

[5]Department of Medicine, Faculty of Medicine, Universidad de Chile, Hospital Clínico Universidad de Chile, Chile

[6]Centre for synthesis and Chemical Biology, University College Dublin, Dublin, Ireland

*Correspondence should be addressed to: JFC. Address: University College Cork, Western Gateway Building, Western Road, Cork, Republic of Ireland. Tel: +353 214205426. E-mail: j.cryan@ucc.ie

Biomaterials. (2014) 35(1):489-99

ABSTRACT

Progression of RNA interference (RNAi)-based gene silencing technologies for the treatment of disorders of the central nervous system (CNS) depends on the availability of efficient non-toxic nanocarriers. Despite advances in the field of nanotechnology undesired and non-specific interactions with different brain-cell types occur and are poorly investigated. To this end, we studied the cytotoxic and neuroinflammatory effects of widely-used transfection reagents and modified amphiphilic β-cyclodextrins (CDs). All non-viral vectors formed positively charged nanoparticles with distinctive physicochemical properties. Differential and significant cytotoxic effects were observed among commercially available cationic vectors, whereas CDs induced limited disruptions of cellular membrane integrity and mitochondrial dehydrogenase activity. Interestingly, murine derived BV2 microglia cells and a rat striatal *in vitro* model of Huntington's Disease (ST14A-HTT120Q) were more susceptible to toxicity than human U87 astroglioma cells. BV2 microglia presented significant increases in cytokine, toll-like receptor 2 and cyclooxygenase-2 gene expression after transfection with selected commercial vectors but not with CD.siRNA nanoparticles. Non-viral short interfering RNA (siRNA) nanoparticles formulated with G6 polyamidoamine (PAMAM) dendrimers also significantly increased cytokine gene expression in the brain following injections into the mouse striatum. Together our data identify modified CDs as nanosystems that enable siRNA delivery to the brain with low levels of cytotoxicity and immunological activation.

Keywords. Cyclodextrins, siRNA, cytokines, toll-like receptors, stereotaxic, High Content Analysis

INTRODUCTION

Therapeutic gene silencing by harnessing the specificity of the endogenous RNA interference (RNAi) pathway offers great promise for the treatment of neurological disorders, such as Huntington's Disease (HD) (Sah, 2006). However, the lack of efficient and safe delivery vectors has tempered the progression of this technology for the treatment of disorders of the central nervous system (CNS) (O'Mahony et al., 2013a). To date, both viral and non-viral approaches have been investigated. Despite their ability to transduce a wide range of cell types, several concerns have been raised against viral vectors regarding their immunogenicity and safety (Thomas et al., 2003). On the other hand, efforts in the field of nanotechnology have been put together to develop more effective and safe non-viral alternatives for short interfering RNA (siRNA) delivery to the CNS (O'Mahony et al., 2013a).

Non-viral vectors are chemically synthesised or derived from naturally occurring polymers and often contain cationic moieties that facilitate electrostatic interaction with anionic siRNAs, enabling complexation and protection from serum degradation (O'Mahony et al., 2013a). These nanosystems have been able to successfully deliver siRNA and elicit gene silencing effects in a variety of cell models, including cultured neurons, but also *in vivo* in the brain of relevant models of CNS disorders (e.g. (Badaut et al., 2011; Godinho et al., 2013; O'Mahony et al., 2012; Wang et al., 2005)). However, and in addition to cellular uptake and gene silencing requirements, biocompatibility of non-viral formulations is one of the emerging hurdles (Ballarín-González et al., 2012). Although until recently biomaterials were considered to be relatively inert, advancements have shown that they are capable of causing toxic biological responses and inducing specific genomic signatures (Akhtar et al., 2007; Ballarín-González & Howard, 2012). Indeed, several delivery vectors (e.g. formulations containing cationic/neutral lipids, cationic linear and branched polymers, polyamidoamine (PAMAM) dendrimers) have been reported to cause cellular membrane destabilization and lysis, and to interfere with mitochondrial metabolic activity leading to increased cellular oxidative stress (Hong et al., 2006; Hunter et al., 2010; Lee et al., 2009; Moghimi et al., 2005). Furthermore, global changes in gene expression profiles, activation of the apoptotic pathway and induction of immune responses have also been reported to occur in a vector-dependent fashion both *in vitro* and *in vivo* upon systemic delivery

(Bonnet et al., 2008; Gorina et al., 2009; Hollins et al., 2007; Hunter & Moghimi, 2010; Kedmi et al., 2010; Omidi et al., 2005).

Key contributors to the toxicological and immunological profiles of nanoparticles are the physicochemical properties of the assembled nanosystem as well as tissue and cell susceptibility (Albanese et al., 2012; O'Mahony et al., 2013a). In fact, surface functionalization, shape, size, charge, and architecture are fundamental aspects for cellular uptake and gene silencing efficiency, and have now been found to be also crucial in nanoparticle-mediated toxicity (Albanese et al., 2012; Gary et al., 2011; Rejman et al., 2004). On the other hand, as ultimate targets in the CNS, neurons are notoriously difficult to transfect and are also very sensitive to cytotoxicity mediated by non-viral vectors (Krichevsky et al., 2002; Tönges et al., 2006). In addition, neurodegenerative diseases, such as HD, may render specific neuronal populations more susceptible to toxic stimuli and therefore adequate non-toxic carriers must be used (Rigamonti et al., 2000). Furthermore, inducing gene silencing effects in the brain requires, in various circumstances, interaction of nanoparticles with different cell types, including microglia and astroglia. Thus, non-specific toxic interactions with these cell types may reduce brain homeostasis, induce inflammatory processes and eventually accelerate progression of neurological diseases (Amor et al., 2010). However, despite its importance, the nanotoxicological and neuroinflammatory impact of nanoparticles for gene and RNAi in the intricate context of the CNS is still relatively poorly investigated. In fact, most studies have focused on single CNS cell types, essentially providing efficacy data and only presenting limited data on the cytoxicity and inflammatory profiles of delivery systems. Thus, a systematic and integrated assessment of the cytotoxic and neuroinflammatory effects of commonly used transfection reagents in multiple brain-derived cells is warranted.

To this end the present study aims to assess the toxicological and immunological profiles of three commercially available and widely used cationic vectors and a modified cationic amphiphilic cyclodextrin (CD) delivery system. These biomaterials were chosen on the basis of their particular molecular architecture and/or in order to cover the most widely used polycation-based delivery systems. Potential biological adverse effects and neuroinflammatory responses were assessed in three

different brain-derived cell lines: ST14A-HTT120Q cells derived from rat striatal primordia and previously cloned with the mutant Huntingtin (HTT) gene were chosen as we are interested in developing non viral therapeutic approaches for HD (Godinho et al., 2013); mouse BV2 microglial cells were chosen as model of CNS resident immune cells; and U87 human astroglioma cells were chosen as brain cancer *in vitro* model. Moreover, we investigated local immune responses to these distinctive biomaterials *in vivo* after single bilateral injections into the striatum of mice.

MATERIALS AND METHODS

Synthetic siRNAs

Synthetic duplexed siRNAs were obtained from QIAGEN (United Kingdom) or Sigma-Aldrich (France). Non-silencing siRNAs (NSsiRNA): sense strand, 5'-UUCUCCGAACGUGUCACGUdTdT-3'; antisense strand, 5'-ACGUGACACGUUCGGAGAAdTdT-3'. Non-silencing FAM-labelled siRNA (FAMsiRNA): sense strand, 5'-[6FAM] UUCUCCGAACGUGUCACGUdTdT-3'; antisense strand, 5'-ACGUGACACGUUCGGAGAAdTdT-3'. HTT siRNAs as per Wang *et al*. 2005 (Wang et al., 2005): 5'-GCCUUCGAGUCCCUCAAGUCC-3'; antisense strand, 5'-ACUUGAGGGACUCGAAGGCCU-3.

Nanoparticle preparation and characterisation

Modified cationic amphiphilic CDs were prepared as previously described in O'Mahony *et al.* (O'Mahony et al., 2012) and Godinho *et al.* (Godinho et al., 2013). Briefly, CDs were dissolved in chloroform and evaporated under a stream of gaseous nitrogen. CDs were then rehydrated in sterilised deionised water (DIW) and sonicated for 1 hour before complexation with siRNAs. For nanoparticle formation, CDs were mixed with equal volumes of siRNA solutions and left to incubate at room temperature (RT) for 20 minutes. Commercially available cationic vectors, Lipofectamine™2000 (Lf2000) (Invitrogen, Carlsbad, CA), INTERFERin® (Interferin) (PolyPlus®, France) and Superfect® (SF) (QIAGEN, United Kingdom) were complexed with siRNAs as per manufacturer's instructions. CD.siRNA nanoparticles were used at a mass ratio 10:1 (10 µg CD : 1 µg siRNA). The final vector/siRNA ratios for commercially available transfection reagents were selected or adapted from manufacturer's recommendations to facilitate comparisons across vectors *in vitro* and also to facilitate comparison with *in vivo* studies (Lf2000 (1 µL Lf2000 : 20 pmol siRNA), SF (5 µL SF : 1 µg siRNA) and Interferin (1-1.2 µL Interferin : 0.1-0.2 µg siRNA). For physicochemical characterisation all nanoparticles were prepared in sterilised DIW and further diluted in DIW up to 1 mL. Size and charge measurements were assessed at RT by dynamic light scattering (DLS) and electrophoretic light

scattering, respectively, using a Malvern's Zetasizer Nano ZS as previously described in O'Mahony *et al.* (O'Mahony et al., 2012) and Godinho *et al.* (Godinho et al., 2013). Results are expressed in mean ± standart deviation (DS) of 3 independent experiments. For *in vivo* studies nanoparticles were prepared in 5% glucose solution (Sigma-Aldrich, Germany) and CD.siRNA nanoparticles concentrated by ultrafiltration using Vivaspin 500 spin columns (Sartorius, Germany) to a final concentration of siRNA of 0.08 µg/µL.

Cell culture and RNAi transfection

ST14A-HTT120Q cells derived from rat striatal primordia and cloned with the human HTT gene were obtained from Coriell Institute for Medical Research (Camden, NJ). BV2 cells derived from primary mouse microglia cells were obtained from Banca Biologica e Cell Factory – IST (Italy, Genova). U87 astroglioma cells were a kind gift from Dr. Paul Young (University College Cork). ST14A-HTT120Q cells were cultured in Dulbecco's Modified Eagle Medium (DMEM) (Sigma, St. Louis, MO) supplemented with 10% Fetal Bovine Serum (FBS) (Sigma, Germany). BV2 cells were maintained in Roswell Park Memorial Institute medium 1640 (RPMI) (GIBCO, United Kingdom) medium supplemented with 10% FBS and 2 mM L-glutamine (GIBCO, United Kingdom). U87 cells were grown in DMEM supplemented with 10% FBS and 2 mM L-glutamine (GIBCO, United Kingdom). For passaging ST14A-HTT120Q and U87 cells 0.05% Trypsin-EDTA (GIBCO, United Kingdom) was used, for passaging BV2 cells 0.25% Trypsin-EDTA (Sigma, United Kingdom) was used. All cultures were kept in a humidified incubator with 5% CO2 and at 33 ℃ (ST14A-HTT120Q) or 37 ℃ (BV2 and U87). ST14A-HTT120Q, BV2 and U87 cells were seeded in 96-well plates at a density of 7.5×10^3, 1×10^4 and 1×10^4 cells / well, respectively. For experiments carried out on 12-well plates cells were seeded at a density of 1.7×10^5, 0.3×10^6, and 2×10^5 cells / well, respectively.

RNAi transfection or stimulation with lipopolysaccharide (LPS) (Sigma, Germany) was carried out for 4, 24 or 48 hours according to the experiment. Nanoparticles were prepared as described above and diluted in optiMEM®. The volume of transfection sample accounted for 20% of the total volume

of the well, the remaining 80% consisted of complete growth media. The final concentration of siRNA in all RNAi-treated groups was of 100 nM.

Trypan blue exclusion assay

The trypan blue assay is a well established method for the evaluation of cell viability in cell suspensions (Kepp et al., 2011). This is a dye exclusion assay technique whereby viable cells, with intact cellular membranes, exclude the dye and nonviable cells incorporate the dye (Kepp et al., 2011). The method was conducted essentially as previously described in O'Mahony *et al.* (O'Mahony et al., 2012). Briefly, cells were seeded in 12-well plates and transfected as described above. After 24 hours cell supernatants were collected, spun down, decanted into new tubes and stored at -80 ºC. Cells were washed with phosphate buffered saline (PBS) (Sigma, United Kingdom) and detached using 0.25% trypsin-EDTA (Sigma, United Kingdom). Cell suspensions were spun down at 1,000 revolutions per minute (rpm) for 5 minutes and the supernatant decanted. Cell pellet was resuspended in 1 mL of respective growth media. A 1:1 dilution of the cell suspension in a trypan blue solution 0.4% (Sigma, United Kingdom) was carried out, and cell counts (total and living cells) were obtained from BioRad TC10™ Automated Cell Counter.

Lactate Dehydrogenase release assay

Lactate Dehydrogenase (LDH) release assay measures early and even transient damages to the cellular membrane (Kepp et al., 2011). An increased leakage of cytosolic LDH to the cell supernatant has been associated with an increase in cytototoxicity (Kepp et al., 2011). LDH assay was carried out on cell supernatants using CytoTox® 96 Non-radioactive Cytotoxicity Assay from Promega (Madison, WI) as per manufacturer's instructions. Briefly, cell supernatants were defrosted on ice and 50 µL of each sample was placed in triplicate on 96-well plates and respective complete media used as control. 50 µL of substrate solution was added into each well and incubated at RT for 30 minutes protected from light. 50 µL of stop solution was added to each well and absorbance measured at 490 nm using a SpectraMax Plus384 plate reader.

Methyl thiazolyl tetrazolium assay

Methyl thiazolyl tetrazolium (MTT) (3-(4,5-dimethylthiazol-2-yl)-2,5-diphenyltetrazoliumbromide) (Sigma, St. Louis, MO) assay assesses mitochondrial reductase activity and therefore is a good measure of cellular metabolism (Kepp et al., 2011). Reduction in mitochondrial dehydrogenase activity has been associated with reduced cell viability. MTT assays were carried out in 96-well plates as previously described in Godinho *et al*. (Godinho et al., 2013) and O'Mahony *et al*. (O'Mahony et al., 2012).

Cell Integrity Assay by High Content Analysis

High Content Analysis (HCA) is a high throughput technique that allows for screening of multiple cellular features based on automated cell imaging analysis. In this study, Cytiva™ Cell Integrity HCA Assay was used to investigate different cell viability parameters such as plasma membrane integrity, mitochondrial viability and apoptosis (Cat. #. 29-0244-69, GE Healthcare, UK). Briefly, dye cocktails containing membrane permeable / impermeable DNA, mitochondrial and phosphatidylserine dyes were prepared following manufacturer's instructions. Cells incubated with Ionomycin 20 µM for 2 hours were validated and included as positive control for cytotoxicity and apoptosis. Three images per well were acquired using the IN Cell Analyser 1000 (GE Healthcare, United Kingdom) with a 20x objective. Further information on excitation and emission wavelengths used for detection of each dye is described in Supplementary Information (SI), Supplementary Materials and Methods. After acquisition, data were analysed using In Cell® 1,000 Workstation software (GE Healthcare, United Kingdom) using multitarget analysis. Specific details on the settings used for analysis are given in SI, Supplementary Materials and Methods.

Gene expression

RNA was isolated using GenELUTE™ Mammalian Total RNA Miniprep Kit (Sigma, St. Louis, MO). 300 ng of total RNA was reverse transcribed to complementary DNA (cDNA) using the High-capacity cDNA reverse transcription kit from Life technologies, Applied Biosystems (Foster City, MO). Real-

time quantitative Polymerase chain reaction (RT-qPCR) was performed using a 7300 Real Time Polymerase chain reaction (PCR) system under the cycling conditions previously described in Godinho *et al*. (Godinho et al., 2013). Mouse Tumour Necrosis Factor (TNF)-α (Mm00443258_m1), Interleukin (IL)-1β (Mm00434228_m1), IL-6 (Mm00446190_m1), Toll-like receptor (TLR) 2 (Mm00442346_m1), cyclooxygenase 2 (COX-2) (Mm00478374_m1) and β-actin (4352341E) Taqman® gene expression assays were acquired from Life technologies, Applied Biosystems (United Kingdom). Custom TaqMan® HTT FAM-labelled probe was designed on previously validated primers as per Godinho *et al.* (Godinho et al., 2013). Samples were run in triplicate and average CT values were used for gene expression calculations. β-actin gene expression was used as endogenous control and relative cytokine gene expression was calculated on normalized CT values.

Brain stereotaxic surgery

Bilateral injections into the striatum (CPu) of 6-week old C57/BL6 male mice (Harlan, United Kingdom) were carried out through brain stereotaxic surgery. Previously optimised coordinates from bregma were used (Anterior-posterior = + 0.7, Medio-lateral = ± 2.0 and Ventral = - 3.0) and a total volume of 2.5 µL was delivered bilaterally at a rate of 0.5 µL/min. In RNAi treated animals 0.2 µg of siRNA was delivered in each side and in positive control animals LPS (3 µg) was injected. Following the injection 5 minutes extra were given before the syringe was retracted to avoid flush back. Bone wax (ETHICON, Johnson&Johnson, Belgium) was used to cover the burr hole and sterile sutures (ETHICON Mersilk, Belgium) were used to sew the skin. All procedures were conducted under gaseous anaesthetic Isofluorane (IsoFlo®, Abbott, United Kingdom). After 24 hours animals were euthanized and brain tissue collected using a brain slicer matrix. Tissue for western blotting was snap frozen in dry ice and tissue for gene expression analysis was kept in RNA later (Sigma, United Kingdom) at 4 ºC overnight. All tissues were thereafter kept in -80 ºC until further analysis. All animal experimental procedures were approved by the ethical committee at the University College Cork and performed in accordance with the European Union directive 2010/63/EU for animals used for scientific purposes.

Western blotting

Brain tissue from the site of injection was disrupted by homogenization in lysis buffer and total protein quantified using a bicinchoninic acid assay as described in Godinho *et al.* (Godinho et al., 2013). 30 µg of total protein was loaded on NuPAGE Novex 4-12% Bis-Tris gel (Invitrogen, Carlsbad, CA). Protein electrophoresis, protein transfer to a polyvinylidene difluoride (PVDF) membrane (Millipore, Bedford, MA) and membrane blocking was carried out as described in Godinho *et al*. (Godinho et al., 2013). Membranes were incubated overnight with anti-Glial Fibrillary Acidic Protein (GFAP) antibody (dilution 1:1,000) (MAB3402, Millipore, Temecula, CA) or anti-β-actin (dilution 1:3,000) (A5441, Sigma, St Louis, MO). Membrane was washed with Tris-buffered saline solution containing 0.1% Tween 20 (Fisher Scientific, Fair Lawn, NJ) and incubated for 1 hour with anti-mouse antibody (dilution 1:10,000) (IRDye 800CW, LI-COR). LICOR Odyssey near-infrared scanner was used to scan membranes and ImageJ software to carry out densitometry analysis. All results were normalised to the house keeping gene β-actin.

Statistical analysis

Unless otherwise stated results are expressed as mean ± standard error of mean (SEM). One-way analysis of variance (ANOVA) followed by Bonferroni's Post Hoc test was carried to determine statistical significant differences in particle size and surface charge among all non-viral vectors. ANOVA followed by Dunnett's Post Hoc test was used to determine significant statistical differences between naked siRNA, CD, Lf2000, Interferin and SF against untreated controls. Student's t-tests were carried out to investigate significant differences between LPS-positive controls and untreated controls. In *in vivo* studies statistical significant differences were investigated against vehicle, whereas untreated animals were only kept as a reference. All statistics were carried out using PAWS 18 Statistical package.

RESULTS

Physicochemical characterisation of non-viral siRNA nanoparticles

The non-viral delivery systems investigated in this study have been represented in Figure 1a. Cationic amphiphilic CDs are siRNA nanocarriers consisting of click-modified β-CDs (Godinho et al., 2013; O'Mahony et al., 2012). On the other hand, Lf2000 consists of a cationic liposome formulation (3:1 DOSPA:DOPE (Fiszer-Kierzkowska et al., 2011; Vangasseri et al., 2006)), Interferin is a proprietary cationic non-liposomal amphiphile and SF is a 6^{th} generation fractured PAMAM dendrimer (Hollins et al., 2007). Lf2000, Interferin and SF are commercially available and have been widely used for nucleic acid transfection. Although all cationic vectors were able to successfully bind and complex siRNAs as shown in gel retardation assays (Figure 1b), the hydrodynamic radius, polydispersity and surface charge of these non-viral siRNA nanoparticles varied significantly (Figure 1c,d). CD (192.34 ± 9.89 nm) and Lf2000 siRNA nanoparticles (222.37 ± 4.96 nm) were significantly larger than Interferin (122.83 ± 7.86) and SF (148.81 ± 16.33). Furthermore, polydispersity index (PDI) of these nanoparticles decreased in the following order CD (0.329 ± 0.033) > Interferin (0.173 ± 0.038) > SF (0.129 ± 0.048) > Lf2000 (0.071 ± 0.007), suggesting different degrees of homogeneity within samples. Finally, zeta potential measurements demonstrated that all non-viral siRNA nanoparticles were positively charged and that CD.siRNA nanoparticles presented the lowest surface charge. However, no statistically significant differences were found among the different systems (Figure 1d).

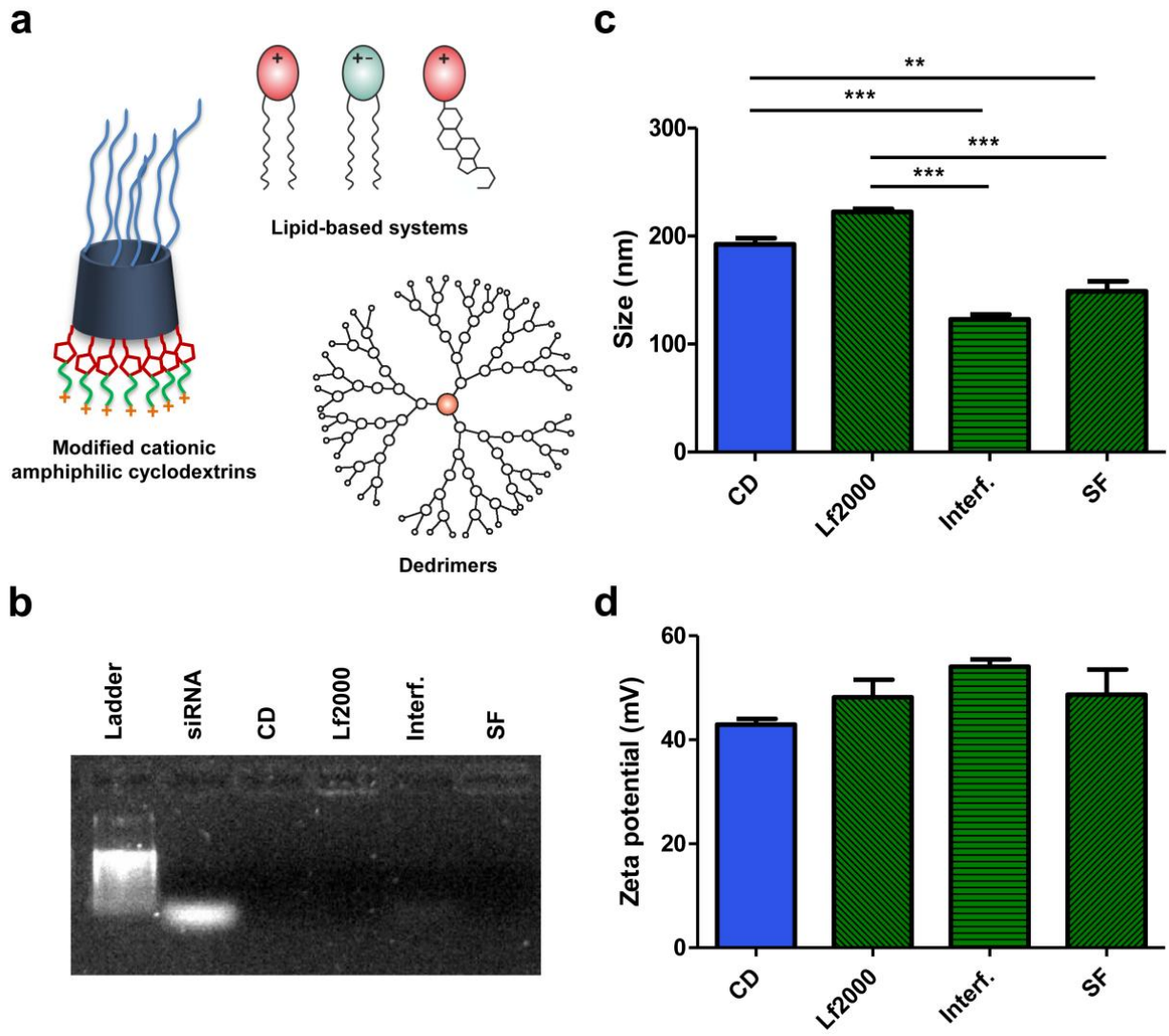

Figure 1. Physicochemical characterisation of non-viral siRNA nanoparticles. *(a) Schematic representation of non-viral vectors. (b) Gel retardation assay for siRNA binding and complexation. Free siRNA migrates through the gel. 0.3µg siRNA per well. (c) Hydrodynamic radius of non-viral siRNA nanoparticles measured by DLS. (d) ζ potential measured through electrophoretic light scattering. Results are expressed as Mean ± SD. **P<0.01 and *** P<0.001. n = 3 per group.*

Gene silencing efficiency in ST14A-HTT120Q cells

For completion and to enable further comparison among the different vectors their gene silencing efficiency was investigated in ST14A-HTT120Q cells, an *in vitro* model of HD. Transfection with Lf2000 and Interferin induced the highest levels of HTT gene expression knockdown in this cell line (Table 4.1). Furthermore, CD.siRNA nanoparticles also induced a very high level of HTT gene expression knockdown, whereas SF was the nanosystem that achieved the lowest level of gene expression knockdown in this cell line (Table 4.1).

Table 1. HTT gene expression knockdown efficiency of non-viral vectors in ST14-HTT120Q cells

Non-viral delivery system	HTT gene expression knockdown (% of untreated controls)
Cyclodextrin	45.06 ± 16.49
Lipofectamine®2000	69.90 ± 6.42
INTERFERin®	63.74 ± 12.13
Superfect®	29.25 ± 6.80

Direct biological adverse effects of non-viral siRNA nanoparticles in brain-derived cell lines

Assessment of direct biological adverse effects using conventional end-point methods revealed differential toxicity profiles of non-viral siRNA nanoparticles within the same brain-derived cell line. Moreover, trypan blue exclusion assays (Figure 2a–c), LDH assays (Figure 2d–f) and MTT assays (Figure 2g–i) provided insights into the various aspects of cellular toxicity. Trypan blue dye exclusion assays provided robust live/dead cell evaluation based on permanent cellular membrane damage, LDH assays detected transient and early injury to the cellular membrane and MTT assays were used as a measure of cellular metabolic activity (Jurisic et al., 2008; Kepp et al., 2011; Lappalainen et al., 1994).

In the rat striatal cell line (ST14A-HTT120Q) siRNA transfections using Lf2000 and Interferin resulted in significant reduction in cell viability (53.2 ± 3.1% and 37.6 ± 7.5% viable cells after 24 hours, respectively), increased LDH release (4.08 ± 0.08 and 5.06 ± 0.39 fold-increase after 24 hours, respectively) and reduction in mitochondrial dehydrogenase activity (46.29 ± 0.53%, 76.36 ± 2.39% metabolically active cells after 48 hours, respectively) (Figure 2a,d,g). Although after 24 hours transfection SF.siRNA nanoparticles did not affect cell viability or LDH release, they had significant effects in mitochondrial metabolic activity after 48 hours (71.72 ± 0.54%). No significant adverse effects were detected for CD.siRNA nanoparticles in all toxicity tests carried out in ST14A-HTT120Q cells (Figure 2a,d,g).

Interferin and SF siRNA nanoparticles significantly reduced cell viability (56.47 ± 5.29% and 43.88 ± 1.44% viable cells after 24 hours, respectively), increased LDH release (2.59 ± 0.06, 2.93 ± 0.08 fold-increase after 24 hours, respectively) and reduced dehydrogenase activity (12.60 ± 1.85%, 53.13 ±

4.00% metabolically active cells after 48 h, respectively) in BV2 microglia cells (Figure 2b,e,h). Although Lf2000 did not reduce cell viability, it significantly increased LDH release after 24 hours (2.10 ± 0.084 fold-increase) and reduced dehydrogenase activity (36.78 ± 2.97% metabolically active cells) after 48 hours. On the other hand, CD.siRNA nanoparticles only modestly affected cellular metabolic activity (79.59 ± 6.13% metabolically active cells) in BV2 cells after 48 hours (Figure 2b,e,h).

Although not dramatically, Lf2000 and interferin siRNA nanoparticles significantly reduced cell viability (92.09 ± 1.50% and 92.43 ± 1.91% viable cells after 24 hours transfection, respectively) and increased LDH release (3.13 ± 0.51% and 3.85 ± 0.30 fold-increase after 24 hours, respectively) in U87 astroglioma cells (Figure 2c,f,i). However, after 48 hours Interferin.siRNA nanoparticles did not induce significant changes in mitochondrial metabolic activity in this cell line whereas Lf2000 did (81.50 ± 0.63% metabolically active cells). Although no changes were observed in trypan blue and LDH assays after 24 hours, SF.siRNA nanoparticles induced mitochondrial adverse effects detected by MTT assay after 48 hours (47.39 ± 0.70% metabolically active cells). No toxic effects in U87 cells were observed with CD.siRNA nanoparticles in the tests performed (Figure 2c,f,i). Trypan blue dye exclusion assays, LDH and MTT biochemical assays did not detect any detrimental effects of naked siRNAs in the brain-derived cell lines tested in this study.

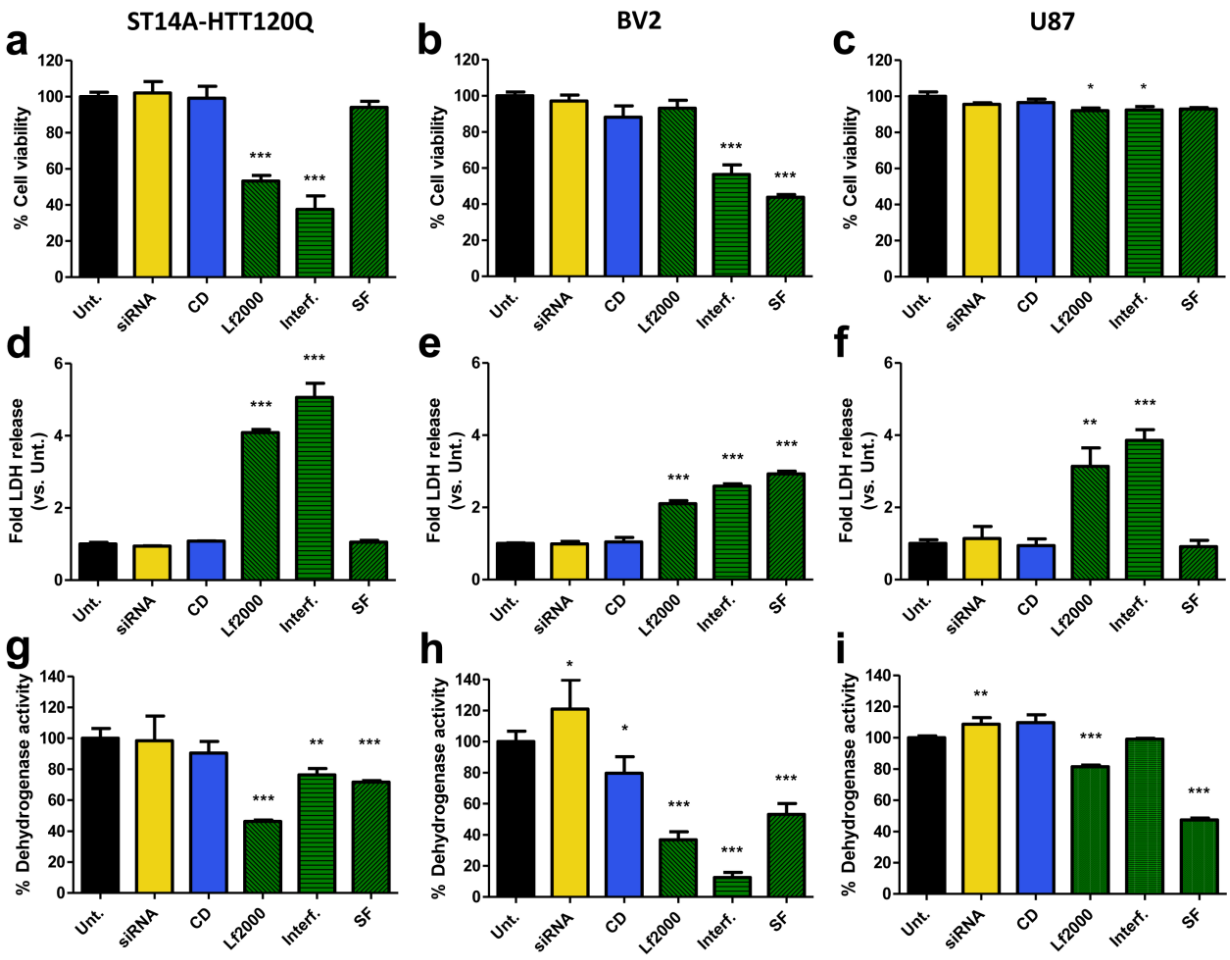

Figure 2. Evaluation of nanoparticle-induced cytotoxicity in multiple brain-derived cell lines using conventional methods. *ST14A-HTT120Q cells (a, d, g), BV2 microglial cells (b, e, h) and U87 cells (c, f, i) were transfected using different non-viral siRNA nanoparticles. Final concentration of siRNA in RNAi-treated groups was of 100 nM for all experiments. Trypan blue exclusion assays (a-c) and LDH release assays (d-f) were carried out after 24 hours of transfection. MTT assays were performed after 48 hours transfection (g-i). Results are expressed as Mean ± SEM. *P<0.05, **P<0.01 and ***P<0.001 against untreated control. n = 3-5 per group.*

HCA was used to further investigate nanoparticle-induced cytotoxicity in the ST14A-HTT120Q *in vitro* model of HD (Figure 3). Figure 3 a shows fused images of the HCA cell integrity assay where membrane permeant nuclear blue stain identifies viable living cells, membrane impermeant red nuclear dye identifies dead cells (co-staining with blue yields magenta), phosphatidylserine green marker identifies apoptotic cells and red mitochondrial stain identifies healthy mitochondria. After 24 hours, Lf2000 and Interferin significantly reduced the number of viable cells (51.61 ± 3.62% and 18.93 ± 5.17% of total number of cells, respectively) and increased the number of late apoptotic

(43.72 ± 2.98% and 71.98 ± 5.48% of total number of cells, respectively) and dead cells (4.68 ± 1.90% and 9.09 ± 2.67% of total number of cells, respectively) (Figure 3 b). In addition, Lf2000 and Interferin also significantly decreased cell density by 45.12 ± 3.32% and 49.86 ± 1.69%, respectively, when compared to untreated controls (Figure 3c). Furthermore, HCA revealed that Lf2000 and Interferin increased membrane permeability by 147.80 ± 5.17% and 241.60 ± 8.69%, respectively, when compared to untreated controls following cellular insult (Figure 3d). Despite obvious differences in sensitivity, these results are in accordance with trypan blue and LDH assays, respectively. Nuclear morphology analysis showed significant shrinkage of the nuclear area in Lf2000 (-23.49 ± 2.33%) and Interferin (-43.35 ± 0.84%) transfected cells (Figure 3e). Additionally, Lf2000 and Interferin significantly reduced mitochondrial membrane potential (MMP) by 38.4 ± 0.63% and 45.04 ± 2.79%, respectively (Figure 3f). On the other hand, naked siRNAs, CDs and SF did not alter significantly any of the above mentioned cell integrity parameters when compared to untreated controls. However, and in contrast with CDs which have efficiently transfected ST14A-HTT120Q cells in the present study, it is worth noting that the good viability profile observed for SF might have been associated with the lower levels of transfection achieved in this particular cell line. Finally, cells stimulated for 2 hours with a calcium ionophore (Ionomycin 20 µM), known to increase release of intracellular calcium and to induce an apoptotic like process, presented reduction in cell densities, number of viable cells, nuclear area and the MMP. Ionomycin also significantly increased the number of late apoptotic cells and plasma membrane permeability when compared to untreated controls (Figure 3a-f).

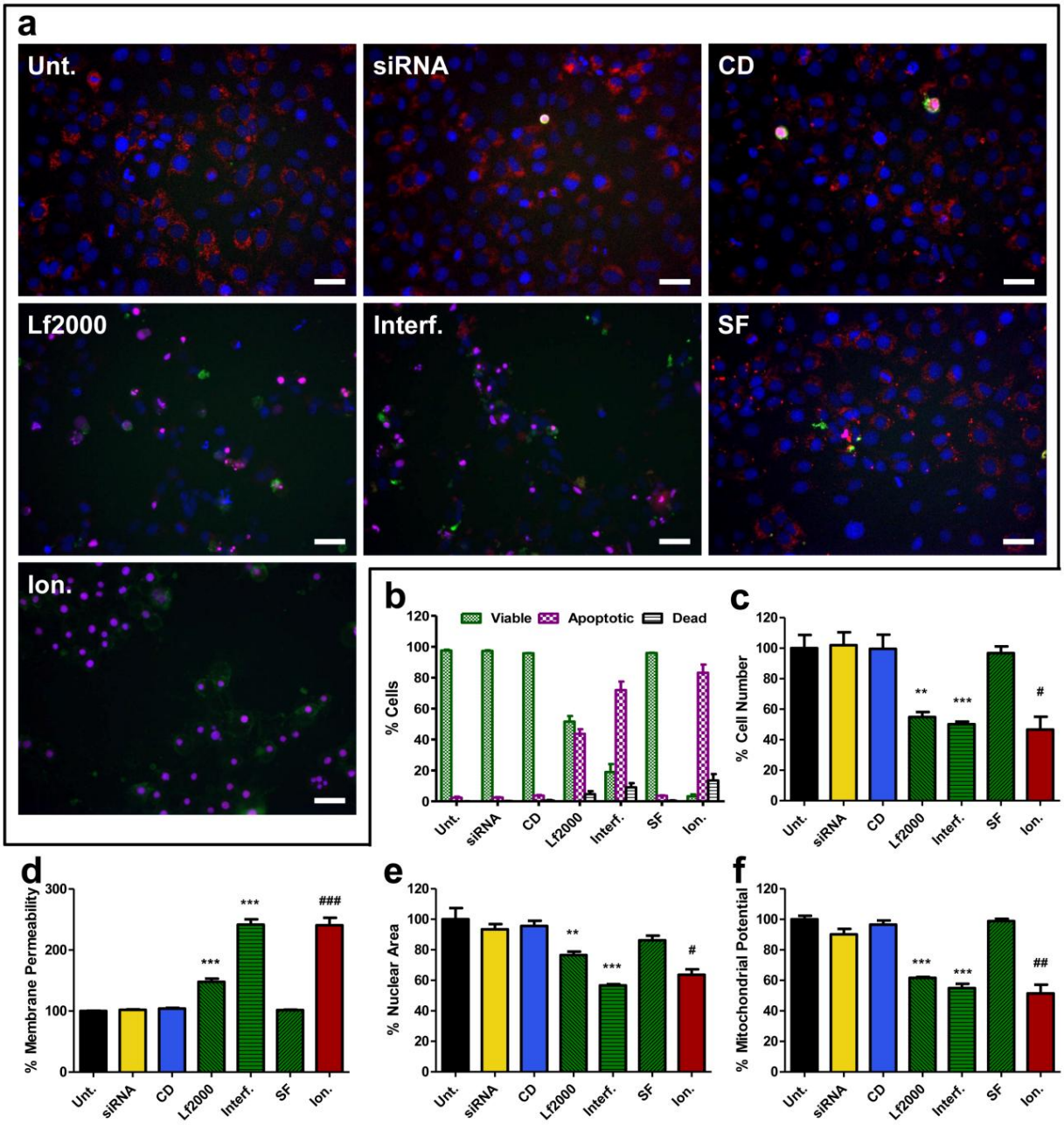

Figure 3. Nanoparticle-induced cytotoxicity in ST14A-HTT120Q striatal cells assessed by High Content Analysis. *ST14A-HTT120Q cells were transfected for 24 h with different non-viral siRNA nanoparticles. Final concentration of siRNA in RNAi-treated groups was of 100 nM. Ionomycin 20 µM incubated for 2 h was used as positive control for apoptosis. (a) Representative fused images obtained from HCA consisting of (blue) nuclear permeant dye indicating viable cells, (red) mitochondrial stain identifying healthy mitochondrion, (green) marker for presence of phosphatidylserine in outer plasma membrane and (magenta) indicating co-localization of blue nuclear stain with membrane impermeant dye, identifying late apoptotic cells. (b) Percentage of viable, apoptotic and dead cells from total cell count. (c) Cell number (d) Membrane permeability (e) Nuclear area and (f) Mitochondrial membrane potential presented as a percentage of untreated controls. Results are expressed as Mean ± SEM. *P<0.05, **P<0.01 and ***P<0.001 against untreated control. n = 3 per group.*

Nanoparticle-induced neuroinflammatory responses in brain-derived cell lines

Immune responses in the CNS are mainly mediated by microglia and astroglia. Therefore here we tested BV2 microglia cells and U87 astroglioma cells for the expression of pro-inflammatory markers, such as cytokines, after transfection with different non-viral vectors.

Results showed that after only 4 hours Lf2000, Interferin and SF siRNA nanoparticles had significantly increased TNF-α gene expression (2.65 ± 0.28, 1.98 ± 0.24, 2.26 ± 0.4 fold-increase, respectively), which was further increased for Interferin and SF (29.59 ± 2.18 and 46.35 ± 2.75, respectively) after 24 hours (Figure 4a). IL-1β gene expression was only found to be significantly increased in cells transfected with SF.siRNA nanoparticles after 4 hours (26.58 ± 11.22 fold-increase), however after 24 hours both Interferin and SF induced significant increases in IL-1β gene expression (225.88 ± 63.65 and 386.51 ± 115.07, respectively) (Figure 4b). In contrast, no significant changes from untreated controls were observed for cells treated with naked siRNA or CD.siRNA nanoparticles for any of the cytokines assessed at any of the time points (Figure 4a,b). A positive control for cytokine release, LPS induced a significant increase in TNF-α and IL-1β gene expression immediately after 4 hours stimulation. The expression of IL-6 was also assessed in this study, yet no expression of this cytokine was detected with either LPS positive control or with the different non-viral vectors (data not shown). For completion of these results we investigated cytokine release to the culture medium in BV2 and U87 cells through multi-spot enzyme-linked immune sorbent assay (ELISA) after 24 hours transfection. In BV2 cells, Lf2000, Interferin and SF significantly increased TNF-α release when compared to untreated controls (2.55 ± 0.11, 1.80 ± 0.48 and 1.54 ± 0.23 pg/mL, respectively), however this was only a modest increase at this particular time point (SI, Supplementary Figure S1). Release of IL-1β in BV2 cells was only found to be modestly increased with LPS and none of the vectors induced significant release of this cytokine (SI, Supplementary Figure S1). In the U87 astroglioma cell line, Lf2000 and Interferin were found to significantly increase release of IL-6 (51.89 ± 6.44, 49.08 ± 7.38 pg/mL, respectively) (SI, Supplementary Figure S1). Moreover, stimulation of U87 cells with LPS resulted in low levels of expression of TNF-α and IL-1β release after 24 hours (data not shown).

The expression of the pattern recognition TLR2 was also assessed and found to be significantly increased in BV2 cells after 4 hours transfection with Lf2000 (3.16 ± 0.14 fold-increase) and Interferin (3.47 ± 0.54 fold-increase) (Figure 4c). Further increases were observed at 24 hours for Interferin (11.73 ± 0.64 fold-increase) and SF siRNA nanoparticles (11.51 ± 1.13 fold-increase). On the other hand, neither naked siRNAs nor CD.siRNA nanoparticles induced significant increases in the expression of this pattern recognition receptor (Figure 4c). Finally, the expression of the pro-inflammatory prostaglandin synthase COX-2 was found to be significantly increased in BV2 cells treated with SF.siRNA nanoparticles (84.25 ± 7.95 fold-increase) (Figure 4d). Despite a modest increase observed with siRNA nanoparticles formulated with CD (2.56 ± 0.90 fold-increase), Lf2000 (2.74 ± 0.56 fold-increase) and Interferin (2.85 ± 0.75 fold-increase) results for these nanoparticles did not reach significance when compared to untreated controls.

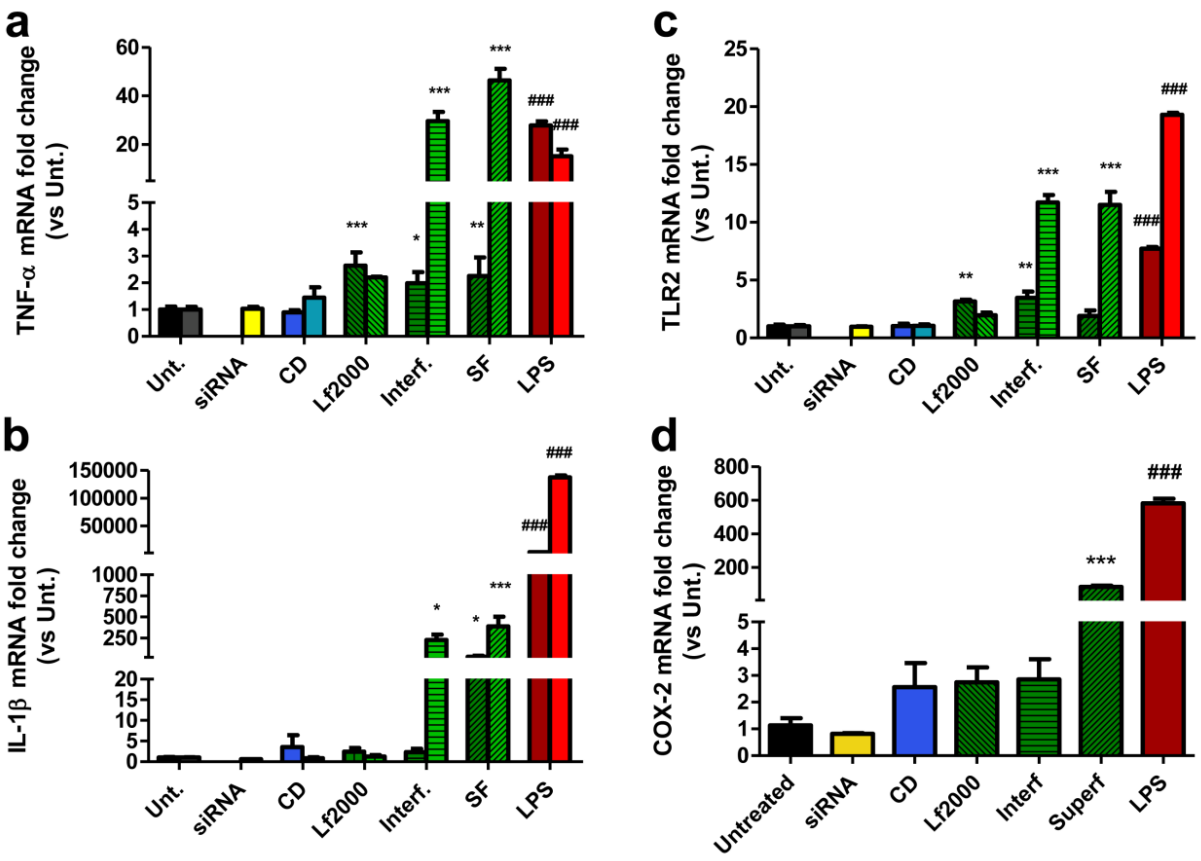

Figure 4. Nanoparticle-induced pro-inflammatory gene expression in BV2 microglia cells. *BV2 microglia cells were transfected for 4 or 24 hours using different nanoparticles. Final siRNA concentration was of 100 nM for all experiments. Total RNA was extracted, reverse transcribed to cDNA and gene expression assessed by RT-qPCR. (a-c) First bar series correspond to gene expression at 4 hours and second bar series to 24 hours. All results were normalized to the expression of β-actin endogenous control. LPS was used as positive control. Results are expressed as Mean ± SEM. *P<0.05, **P<0.01, ***P<0.001 and ###P<0.001 against untreated control. n = 3-5 per group.*

Acute *in vivo* neuroinflammatory responses to non-viral siRNA nanoparticles in the brain

In order to investigate local activation of immune response in the brain caused by non-viral siRNA nanoparticles, direct injections into the striatum of C57/BL6 mice were performed. Subsequently, gene expression of pro-inflammatory cytokines TNF-α, IL-1β and IL-6 gene expression were assessed through RT-qPCR (Figure 5). After 24 hours, all animals subjected to stereotaxic brain surgery revealed an expected increase in the expression of TNF-α due to mechanical lesion and trauma. However, only SF.siRNA nanoparticles significantly increased the expression of this cytokine when compared to vehicle-treated animals (527.40 ± 137.10 fold-increase) (Figure 5a). Furthermore, the

expression of IL-1β was found to be undetectable in untreated control animals and only SF.siRNA nanoparticles significantly increased its expression when compared to vehicle-treated animals (Figure 5b). Finally, expression of IL-6 was found to be significantly enhanced in animals treated with SF.siRNA nanoparticles (259.50 ± 94.54 fold-increase) and a trend towards significance was found for animals treated with Interferin.siRNA nanoparticles (Figure 5c). Naked siRNA did not stimulate the expression of any of the cytokines screened in this study. In contrast, LPS caused a significant and dramatic increase in TNF-α, IL-1β and IL-6 after 24 hours.

Furthermore, astroglia activation was evaluated by assessing GFAP levels across the different treatment groups (Figure 5d box). All animals subjected to brain surgery presented increased levels of GFAP when compared to untreated animals. Although a positive trend towards significance is clear for animals treated with Lf2000 and SF siRNA nanoparticles, no statistical significance was achieved (Figure 5d). Moreover, only modest weight loss was noted in all RNAi-treated animals, except for the SF-treated group where significant differences were observed when compared to vehicle-treated animals (SI, Supplementary Figure S2).

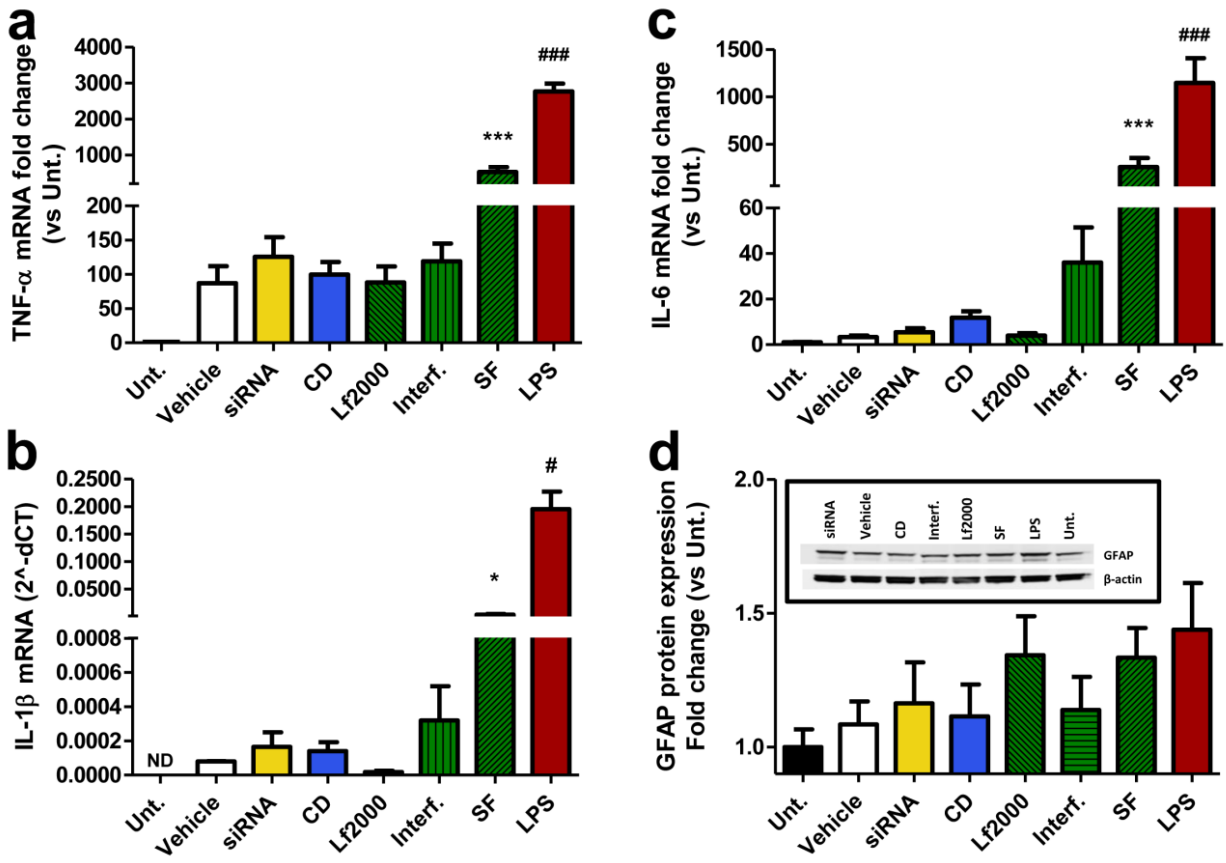

Figure 5. Acute in vivo neuroinflammatory responses to non-viral siRNA nanoparticles in the brain. *Different non-viral siRNA nanoparticles were injected bilaterally (2 x 0.2 µg siRNA / 2.5µL) into the striatum of 6-week old C57/BL6 male mice. After 24 hours, total RNA was extracted, reverse transcribed to cDNA and cytokine gene expression assessed by RT-qPCR (a-c). (d) Western blot (box) and densitometry analysis for GFAP protein expression. LPS was used as positive control. All results were normalized to the expression of β-actin endogenous control. Results are expressed as Mean ± SEM. ***P<0.001 and ###P<0.001 against vehicle control. n = 3-12 per group.*

DISCUSSION

Developing nanosystems for RNAi delivery is a difficult balancing act between inducing an appropriate level of efficacy versus the biocompatibility and safety liabilities of the assembled nanosystem. This is particularly cogent for disorders of the CNS where neuronal and glial cells are highly sensitive to cytotoxic insults. Moreover, the rapid developments in nanotechnology have resulted in the establishment of a wide range of non-viral vectors whose biological and immunological effects in the CNS are still to be comprehensively elucidated and compared. Thus, this report aims to solely evaluate the differential nanotoxicological and neuroinflammatory effects of widely used non-viral vectors for siRNA delivery to the CNS.

The physicochemical characteristics of the assembled nanosystem have been shown to dictate cellular uptake and gene knockdown efficiency, but also their cytotoxic effect. In this study, the different vectors (CD, Lf2000, Interferin and SF) yielded nanoparticles with comparable surface charges but with varying hydrodynamic sizes. Similar particle sizes have been previously reported by our group for CD.siRNA nanoparticles in DLS studies (Godinho et al., 2013; O'Mahony et al., 2012), and further confirmed by morphological studies using transmission electron microscopy (O'Mahony et al., 2013b). Furthermore, vectors achieved different degrees of gene silencing of the mutant HTT gene in an *in vitro* model of HD (ST14A-HTT120Q), with CD.siRNA nanoparticles having a similar potency to that described previously (Godinho et al., 2013). However, and despite the fact that all nanoparticles presented comparable surface charges, only CD.siRNA nanoparticles have consistently presented safer cytotoxic profiles across most cell lines and assays here performed. Thus, in spite of the well documented detrimental effects of high positive surface charges (Bertero et al., 2013; Hong et al., 2006; Hunter, 2006; Kedmi et al., 2010), we suggest that the differences in cytotoxicity and also in the degree of HTT suppression observed, are probably in part associated with other characteristics of the nanoparticles, such as size and/or morphology. Indeed, others have found that nanoparticle size is a key factor in determining the specific cellular uptake and intracellular trafficking pathways whereas nanoparticle morphology may determine selective uptake by neurons and/or microglia (Albanese et al., 2012; Rejman et al., 2004). We also reason that, biodegradability and clearance of the nanosystem

from the intracellular compartment could have played an important role in cellular toxicity, however, further investigations are needed to clarify the mechanisms implicated. On the other hand, it is of interest to note that recent microarray data show that different biomaterials induce cell-specific "gene fingerprints", deregulating various genes related to apoptosis, cell proliferation and differentiation and mechanisms of DNA repair (Choi et al., 2010; Hollins et al., 2007; Merkel et al., 2011; Omidi et al., 2005). In turn, these genomic disruptions significantly differ between empty non-viral vectors and assembled nanosystems (containing their nucleic acid cargo) (Choi et al., 2010; Hollins et al., 2007; Omidi et al., 2005). Therefore, this may suggest that cells recognize assembled nanosystems as singular entities distinct from the individual components, and that pathways implicated in subsequent cytotoxicity may also be different (Akhtar & Benter, 2007).

Inducing gene silencing effects in the brain requires in various circumstances interaction of nanoparticles with different cell types, including neurons and glia (O'Mahony et al., 2013a). Thus, here we emphasise important differences in cellular susceptibility to the toxic stimulus mediated by non-viral vectors in brain-derived cell lines. Our results showed that ST14A-HTT120Q striatal cells and U87 astroglioma cells seemed to be more susceptible to toxic adverse effects from Lf2000 and Interferin siRNA nanoparticles, whereas BV2 microglia cells seemed to be more susceptible to toxicity from Interferin and SF. In agreement with our results, others have found that cellular uptake and cytotoxic profiles of widely used commercially available vectors are largely cell type-dependent (Gebhart et al., 2001; Kiefer et al., 2004; Uchida et al., 2002; Yamano et al., 2010). Furthermore, in the specific context of the CNS, primary cultured astrocytes and microglial cells have also presented differential cellular uptake profiles when transfected with lipid-formulated siRNA (Ki et al., 2010). Together, the differential toxicological cellular responses found in these studies may be related to the specific composition of cellular membranes of each cell-type, differences in the interaction of the biomaterials with intracellular components, but also in how cells are able to process and degrade these biomaterials. Overall, ST14A-HTT120Q cells, an *in vitro* model of HD, and the BV2 microglia cells used in this study seemed to be the most sensitive to adverse effects of non-viral siRNA nanoparticles. Indeed, it has been previously shown that the expression of the mutant and toxic HTT protein in this

striatal cell line renders these cells more prone to toxic insults (Rigamonti et al., 2000). At the other end of the transfection spectrum, U87 astroglia cells, derived from a human astroglioma cancer, seemed to be more resistant to cell death. Thus, the selection of appropriate CNS *in vitro* models and appropriate toxicity assays is crucial for the assessment of biological adverse effects of non-viral vectors.

The majority of studies assessing *in vitro* cytotoxicity of widely used delivery systems have based their biosafety assumptions on a single end-point toxicity assay (e.g. (Gebhart & Kabanov, 2001; Kiefer et al., 2004; Uchida et al., 2002; Yamano et al., 2010)). In fact, despite the vast number of well established toxicity assays available to researchers for monitoring cell death, such as trypan blue exclusion, LDH and MTT assays, there is limited comparative information on the relative utility of these tests (Kepp et al., 2011). In summary, each of the conventional cytotoxicity methods employed in this study assesses a specific parameter involved in cell death and should be used together for a more complete assessment of cytotoxicity. As an example, no dramatic reduction in cell viability was detected in U87 cells upon transfection, nevertheless remarkable increases in LDH release revealed that early disruptions of membrane permeability might be occurring. Furthermore, MTT assays complement these results demonstrating that nanoparticles have also altered mitochondrial metabolic activity significantly. Thus, assumptions regarding biocompatibility of nanomaterials using a single conventional end-point toxicity assay are limited and should be avoided. Alternatively, HCA is a high-throughput technique that allows the evaluation of multiple cellular morphological and biochemical parameters with high sensitivity and specificity (Giuliano et al., 2003). Although this technique is lately becoming popular to assess cytotoxicity of active pharmaceutical compounds (Giuliano et al., 2003), was only recently that HCA has been applied to evaluate efficiency and cytotoxic effects of non-viral vectors for gene delivery and other nanoparticles *in vitro* (Hibbitts et al., 2011; Rawlinson et al., 2010). HCA cell integrity assay revealed that Lf2000 and Interferin siRNA nanoparticles reduced cell densities and the number of viable cells, and increased the number of late apoptotic and dead cells. Presence of phosphatildylserine in the outer face of the plasma membrane and co-staining of the nucleus with nuclear impermeable dye due to increased plasmatic membrane

permeability, enabled identification of these cells as late apoptotic (Van Cruchten et al., 2002). Additionally, RNAi transfection with these vectors induced nuclear contraction and chromatin condensation, both of which are typical features of cells undergoing apoptosis (Rawlinson et al., 2010; Van Cruchten & Van Den Broeck, 2002). Lf2000 and Interferin also triggered loss of MMP indicating that these vectors compromise healthy mitochondrial function, eventually leading to cytochrome C release and induction of several other signalling cascades. Thus, the HCA results bolster our data obtained with conventional methods, however at a much higher degree of sensitivity, while also allowing for specific identification of the cell death mechanism activated by these biomaterials.

Safety of non-viral vectors for RNAi in the CNS is also dependent on a reduced activation of the local immune system. Interestingly, our data showed that the non-viral vectors that induced greater cytotoxic effects in microglia and astroglia cells are more likely to trigger neuroinflammatory responses. Indeed, in BV2 microglia cells, Interferin and SF induced the highest expression of major pro-inflammatory cytokines (TNF-α, IL-1β and IL-6) among all vectors used. Consistent with our results, others have also reported increased cytokine release in primary glial cultures and/or *in vivo*, after systemic administrations, when using lipid- and/or polymer-based siRNA/pDNA nanoparticles (Gautam et al., 2001; Gorina et al., 2009; Sakurai et al., 2002). In addition, although these immunostimulatory effects could have been triggered by the nucleic acid cargo itself rather than the biomaterial, other studies have highlighted that this might be a vector-dependent effect. Indeed, these studies demonstrate that delivery of the same nucleic acid cargo (including unmodified siRNAs) by different vectors leads to differential immune responses after intravenous injection (i.v.) (Bonnet et al., 2008; Kawakami et al., 2006; Kedmi et al., 2010). Thus, certain vectors seem to be more likely to enhance the immunostimulatory effects of siRNA than others, and these effects have been suggested to be closely related to sequestration of siRNA within a TLR7 rich environment in the endosomes (Ballarín-González & Howard, 2012). This further supports the need to develop non-viral vectors with endosomolytic properties and with low cytotoxic effects. Furthermore, it has also been recently suggested that the induction of cytokine expression by nanoparticles and biomaterials may occur through the activation of TLRs (Hutter et al., 2010; Kedmi et al., 2010). Investigations in various

denditric cell models have demonstrated that this is likely to be a structural activity dependent-effect and therefore specific to certain lipids (Lonez et al., 2009; Tanaka et al., 2008; Vangasseri et al., 2006). Although not in the particular context of RNAi or gene delivery, several biomaterials and delivery systems (e.g. PAMAM dendrimers) have been shown to activate microglia, resident immune cells of the CNS, and to increase the expression of specific inflammatory receptors such as TLRs and CC-chemokine receptor 2 (Bertero et al., 2013; Hutter et al., 2010). Expression of TLR2 was found to be enhanced following the administration of Interferin and SF, however further studies are needed to reach a better understanding of the mechanism underlying these effects. Additionally, despite marked increased in cytokine gene expression *in vitro* with SF, Lf2000 and Inteferin, only SF nanoparticles lead to a significant increase gene expression of the pro-inflammatory enzyme COX-2, a key enzyme responsible for the synthesis of prostaglandins. Thus, although expression of COX-2 in the brain is closely regulated by growth factors and cytokines (Ramsay et al., 2003), this differential response of the nanosystems indicates that additional underlying mechanisms are probably responsible for its activation by this G6 PAMAM dendrimer.

Route of administration, length of treatment and dosing regimens have also been identified as important determinants for toxic and inflammatory responses to delivery systems (O'Mahony et al., 2013a). Indeed, here we demonstrate that the mechanical damage during brain intraparenchymal injections *per se* is able to enhance cytokine gene expression and also GFAP levels, effect which is clearly observed in all surgical animals including vehicle-treated animals. In agreement with our *in vitro* data, SF nanoparticles caused significant increases in cytokine gene expression *in vivo* and induced weight loss when compared to vehicle-treated animals. However, in a previous study only moderate glial activation was reported upon intracortical injections with G4 PAMAM dendrimers (Albertazzi et al., 2012). Thus, we speculate that the increased activation of the immune response in our study might be related to the increased cytotoxic effects of the G6 PAMAM dendrimer in the brain. Indeed, *in vitro* mechanistic studies in mammalian cells have demonstrated that dendrimers induce cytotoxic effects in a generation-dependent manner (Mukherjee et al., 2010). On the other hand, although no significant immune activation was found for Interferin in the present *in vivo* study,

increased immunological responses upon brain delivery have been reported elsewhere (Badaut et al., 2011). In contrast, a previous study in our group showed that multiple injections with CD.HTTsiRNA nanoparticles into the striatum of the R6/2 mouse model of HD selectively improved rotarod motor deficits without causing detrimental effects on body weight profiles (Godinho et al., 2013). In addition, other CD-containing polymer delivery systems for siRNA (CALAA-01) have been shown to be well tolerated in non-human primates after multiple i.v. administrations revealing no significant activation of the immune system (Heidel et al., 2007). Therefore, further studies should be carried out for Lf2000, Interferin and SF to assess the effects of multiple injections into this susceptible structure.

CONCLUSION

The functional importance of examining toxicity profiles of nanosystems is obvious when one is extrapolating to *in vivo* analysis. Although brain stereotaxic surgery and direct administration of non-viral siRNA nanoparticles into the CNS is a common practice in research and pre-clinical testing (e.g. (Badaut et al., 2011; Godinho et al., 2013; Wang et al., 2005)), the translation of this approach to the clinic requires a better understanding of the interaction of non-viral siRNA nanoparticles and the CNS cellular milieu. Intrinsic toxicity of nanoparticles might be advantageous when treating brain cancers, but the application of such technologies to neurodegenerative disorders demands low cytotoxic and immunological adverse effects. Thus, taken together our data enable us to identify modified CDs as promising nanocarriers that enable siRNA delivery to the brain with low levels of cytotoxicity and immunological activation.

SUPPLEMENTARY INFORMATION

The SI section includes data regarding nanoparticle-induced cytokine release in brain-derived cell lines (Supplementary Figure S1); body weight changes after stereotaxic injections of different non-viral siRNA nanoparticles into the mouse brain (Supplementary Figure S2); and further details are given regarding materials and methods used in the experimental section (Supplementary Materials and Methods).

Nanoparticle-induced cytokine release in brain-derived cell lines

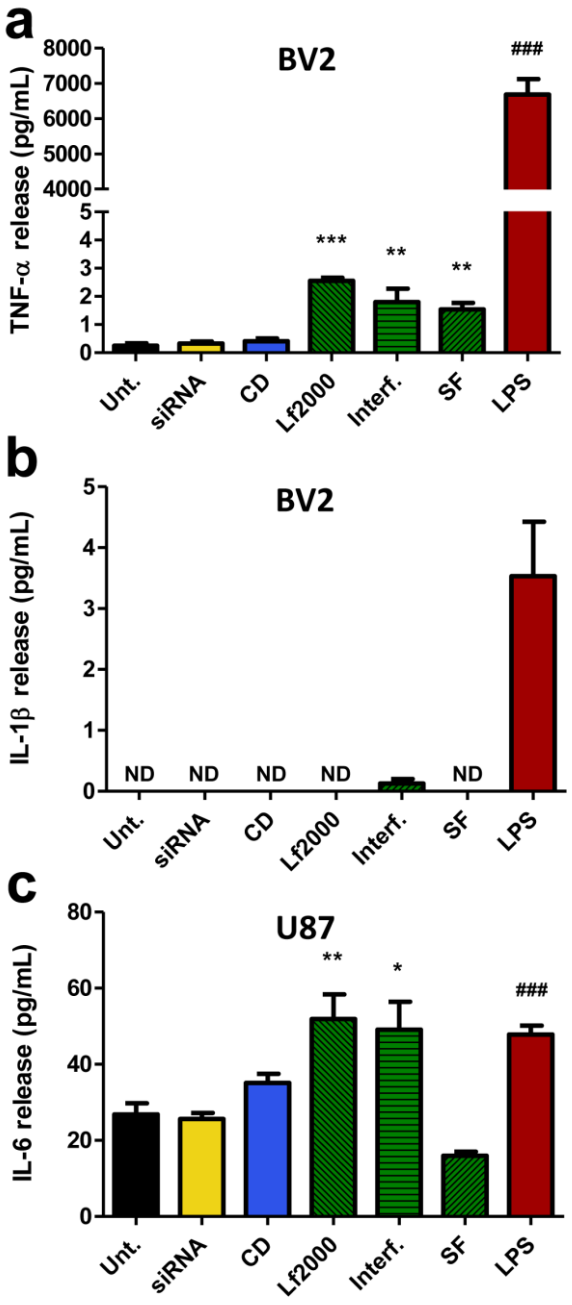

Supplementary Figure S1. Nanoparticle-induced cytokine release in brain-derived cell lines. *BV2 microglia cells and U87 astroglioma cells were transfected for 24 hours using different non-viral siRNA nanoparticles. Final concentration of siRNA in all RNAi-treated groups was of 100 nM. (a-c) TNF-α, IL-1β and IL-6 release to cell supernatants was assessed by using Multi Spot MSD ELISA. LPS was used as positive control. Results are expressed as Mean ± SEM. *P<0.05, **P<0.01, ***P<0.001 and ###P<0.001 against untreated control. n = 3 per group.*

Body weight changes after stereotaxic injections of different non-viral siRNA nanoparticles into the mouse brain

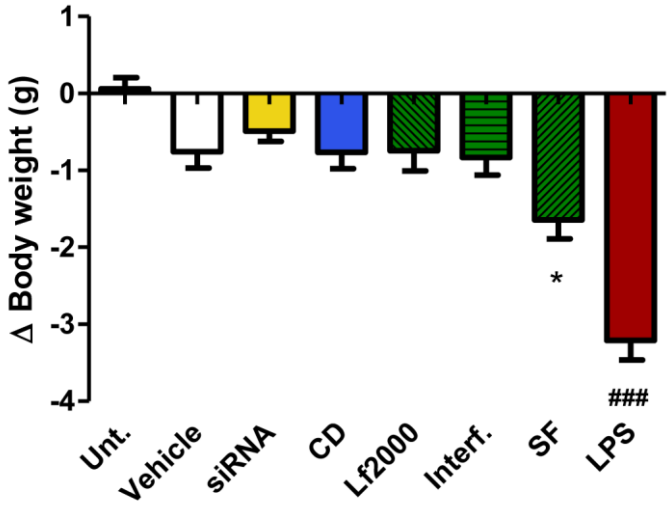

Supplementary Figure S2. Body weight changes after stereotaxic injections of different non-viral siRNA nanoparticles into the mouse brain. *C57/BL6 mice were bilaterally injected into the striatum (2 × 0.2 μg siRNA/2.5 μL) with different non-viral siRNA nanoparticles. Differences in body weights observed 24 hours after stereotaxic injections were recorded. Results are expressed as Mean ± SEM. *P<0.05 and ###P<0.001 against vehicle control. n = 9-11 per group.*

Supplementary Materials and Methods

Cell Integrity Assay by High Content Analysis

Supplementary Table S1. Cytiva™ Cell Integrity Assay kit dye cocktail for HCA assay.

Dye	Excitation/Emission λ (nm)	Dye function	Objects identified
A	360/535	Membrane permeant nuclear stain	All Nuclei
B	535/620	Membrane impermeant nuclear stain	Dead cells nuclei
C	535/620	Membrane permeant indicator for mitochondrial membrane potential	Mitochondria
E	475/535	Phosphatidylserine detection at the plasma membrane	Apoptotic cells

Supplementary Table S2. Multitarget analysis settings cytotoxicity assay analysis with In Cell® 1000 Workstation software.

Object	Source	Segmentation	Others
Nuclei	Wave 1 (360/535)	Top-hat	Min. area: 32 µm^2 / Sensitivity: 90
Cells	Wave 2 (475/535)	Collar	Radius: 7 µm
Reference 1 (dye B)	Wave 3 535/620	Pseudo-nuclei	-
Mitochondria	Wave 3 535/620	Organelles	Multiscale top-hat Range: 1-32 µm Sensitivity: 80 # scales: 3
Reference 2 (dye B)	Wave 3 535/620	Pseudo-cells	-

Cytokine release

BV2 microglia cells and U87 astroglioma cells were transfected for 24 hours with different non-viral siRNA nanoparticles. Cytokine release was assessed from cell supernatants by ELISA. Meso Scale Discovery® (MSD®, Gaithersburg, MD) 96-well plate multi-spot mouse and human pro-inflammatory cytokine assays were purchased for detection of TNF-α, IL-1β, IL-6 and IFN-γ. Mouse assay also included the detection of IL-12p70, IL-10 and KC. Specific manufacturer's instructions were followed for plate preparation. SECTOR® Imager 2400 reader was used to quantify cytokine release.

REFERENCES

Akhtar, S., & Benter, I. (2007). Toxicogenomics of non-viral drug delivery systems for RNAi: potential impact on siRNA-mediated gene silencing activity and specificity. *Adv Drug Deliv Rev, 59*(2-3), 164-182.

Albanese, A., Tang, P. S., & Chan, W. C. (2012). The effect of nanoparticle size, shape, and surface chemistry on biological systems. *Annu Rev Biomed Eng, 14*, 1-16.

Albertazzi, L., Gherardini, M., Sulis Sato, S., Bifone, A., Pizzorusso, T., Ratto, G. M., & Bardi, G. (2012). In vivo distribution and toxicity of PAMAM dendrimers in the central nervous system depend on their surface chemistry. *Mol. Pharm., 10*(1), 249-260.

Amor, S., Puentes, F., Baker, D., & Valk, P. v. d. (2010). Inflammation in neurodegenerative diseases. *Immunology, 129*(2), 154-169.

Badaut, J., Ashwal, S., Adami, A., Tone, B., Recker, R., Spagnoli, D., Ternon, B., & Obenaus, A. (2011). Brain water mobility decreases after astrocytic aquaporin-4 inhibition using RNA interference. *J. Cereb. Blood Flow Metab., 31*(3), 819-831.

Ballarín-González, B., & Howard, K. A. (2012). Polycation-based nanoparticle delivery of RNAi therapeutics: adverse effects and solutions. *Adv Drug Deliv Rev, 64*(15), 1717-1729.

Bertero, A., Boni, A., Gemmi, M., Gagliardi, M., Bifone, A., & Bardi, G. (2013). Surface functionalization regulates PAMAM dendrimer toxicity on Blood Brain Barrier cells and the modulation of key inflammatory receptors on microglia. *Nanotoxicology*(0), 1-11.

Bonnet, M.-E., Erbacher, P., & Bolcato-Bellemin, A.-L. (2008). Systemic delivery of DNA or siRNA mediated by linear polyethylenimine (L-PEI) does not induce an inflammatory response. *Pharm. Res., 25*(12), 2972-2982.

Choi, Y. J., Kang, S. J., Kim, Y. J., Lim, Y.-B., & Chung, H. W. (2010). Comparative studies on the genotoxicity and cytotoxicity of polymeric gene carriers polyethylenimine (PEI) and polyamidoamine (PAMAM) dendrimer in Jurkat T-cells. *Drug Chem. Toxicol., 33*(4), 357-366.

Fiszer-Kierzkowska, A., Vydra, N., Wysocka-Wycisk, A., Kronekova, Z., Jarzab, M., Lisowska, K. M., & Krawczyk, Z. (2011). Liposome-based DNA carriers may induce cellular stress response and change gene expression pattern in transfected cells. *BMC Mol. Biol., 12*, 27.

Gary, D. J., Lee, H., Shama, R., Lee, J.-S., Kim, Y., Cui, Z. Y., Jia, D., Bowman, V. D., Chipman, P. R., Wan, L., Zou, Y., Mao, G., Park, K., Herbert, B. S., Konieczny, S. F., & Won, Y. Y. (2011). Influence of nano-carrier architecture on in vitro siRNA delivery performance and in vivo biodistribution: polyplexes vs micelleplexes. *ACS Nano, 5*(5), 3493-3505.

Gautam, A., Densmore, C. L., & Waldrep, J. C. (2001). Pulmonary cytokine responses associated with PEI-DNA aerosol gene therapy. *Gene Ther., 8*(3), 254-257.

Gebhart, C. L., & Kabanov, A. V. (2001). Evaluation of polyplexes as gene transfer agents. *J. Control. Release, 73*(2-3), 401-416.

Giuliano, K. A., Haskins, J. R., & Taylor, D. L. (2003). Advances in high content screening for drug discovery. *Assay Drug Dev Technol, 1*(4), 565-577.

Godinho, B. M. D. C., Ogier, J. R., Darcy, R., O'Driscoll, C. M., & Cryan, J. F. (2013). Self-assembling modified beta-cyclodextrin nanoparticles as neuronal siRNA delivery vectors: focus on Huntington's Disease. *Mol. Pharm., 10*(2), 640-649.

Gorina, R., Santalucia, T., Petegnief, V., Ejarque-Ortiz, A., Saura, J., & Planas, A. M. (2009). Astrocytes are very sensitive to develop innate immune responses to lipid-carried short interfering RNA. *Glia, 57*(1), 93-107.

Heidel, J. D., Yu, Z., Liu, J. Y. C., Rele, S. M., Liang, Y., Zeidan, R. K., Kornbrust, D. J., & Davis, M. E. (2007). Administration in non-human primates of escalating intravenous doses of targeted nanoparticles containing ribonucleotide reductase subunit M2 siRNA. *Proc Natl Acad Sci USA, 104*(14), 5715-5721.

Hibbitts, A., Lieggi, N., McCabe, O., Thomas, W., Barlow, J., O'Brien, F., & Cryan, S.-A. (2011). Screening of siRNA nanoparticles for delivery to airway epithelial cells using high-content analysis. *Ther. Deliv., 2*(8), 987-999.

Hollins, A. J., Omidi, Y., Benter, I. F., & Akhtar, S. (2007). Toxicogenomics of drug delivery systems: Exploiting delivery system-induced changes in target gene expression to enhance siRNA activity. *J. Drug Target., 15*(1), 83-88.

Hong, S., Leroueil, P. R., Janus, E. K., Peters, J. L., Kober, M.-M., Islam, M. T., Orr, B. G., Baker, J. R., & Holl, M. M. B. (2006). Interaction of polycationic polymers with supported lipid bilayers and cells: nanoscale hole formation and enhanced membrane permeability. *Bioconjug. Chem., 17*(3), 728-734.

Hunter, A. C. (2006). Molecular hurdles in polyfectin design and mechanistic background to polycation induced cytotoxicity. *Adv Drug Deliv Rev, 58*(14), 1523-1531.

Hunter, A. C., & Moghimi, S. M. (2010). Cationic carriers of genetic material and cell death: A mitochondrial tale. *Biochim Biophys Acta, 1797*(6-7), 1203-1209.

Hutter, E., Boridy, S., Labrecque, S., Lalancette-Hébert, M., Kriz, J., Winnik, F. M., & Maysinger, D. (2010). Microglial response to gold nanoparticles. *ACS Nano, 4*(5), 2595-2606.

Jurisic, V., & Bumbasirevic, V. (2008). In vitro assays for cell death determination. *Arch. Oncol., 16*(3-4), 49-54.

Kawakami, S., Ito, Y., Charoensit, P., Yamashita, F., & Hashida, M. (2006). Evaluation of proinflammatory cytokine production induced by linear and branched polyethylenimine/plasmid DNA complexes in mice. *The Journal of Pharmacology and Experimental Therapeutics, 317*(3), 1382-1390.

Kedmi, R., Ben-Arie, N., & Peer, D. (2010). The systemic toxicity of positively charged lipid nanoparticles and the role of Toll-like receptor 4 in immune activation. *Biomaterials, 31*(26), 6867-6875.

Kepp, O., Galluzzi, L., Lipinski, M., Yuan, J., & Kroemer, G. (2011). Cell death assays for drug discovery. *Nat Rev Drug Discov, 10*(3), 221-237.

Ki, K. H., Park, D. Y., Lee, S. H., Kim, N. Y., Choi, B. M., & Noh, G. J. (2010). The optimal concentration of siRNA for gene silencing in primary cultured astrocytes and microglial cells of rats. *Korean J. Anesthesiol., 59*(6), 403-410.

Kiefer, K., Clement, J., Garidel, P., & Peschka-Süss , R. (2004). Transfection efficiency and cytotoxicity of nonviral gene transfer reagents in human smooth muscle and endothelial cells. *Pharm. Res., 21*(6), 1009-1017.

Krichevsky, A. M., & Kosik, K. S. (2002). RNAi functions in cultured mammalian neurons. *Proceedings of the National Academy of Sciences of USA, 99*(18), 11926-11929.

Lappalainen, K., Jääskeläinen, I., Syrjänen, K., Urtti, A., & Syrjänen, S. (1994). Comparison of cell proliferation and toxicity assays using two cationic liposomes. *Pharm. Res., 11*(8), 1127-1131.

Lee, J.-H., Cha, K. E., Kim, M. S., Hong, H. W., Chung, D. J., Ryu, G., & Myung, H. (2009). Nanosized polyamidoamine (PAMAM) dendrimer-induced apoptosis mediated by mitochondrial dysfunction. *Toxicol. Lett., 190*(2), 202-207.

Lonez, C., Lensink, M. F., Vandenbranden, M., & Ruysschaert, J.-M. (2009). Cationic lipids activate cellular cascades. Which receptors are involved? *Biochim Biophys Acta, 1790*(6), 425-430.

Merkel, O. M., Beyerle, A., Beckmann, B. M., Zheng, M., Hartmann, R. K., Stöger, T., & Kissel, T. H. (2011). Polymer-related off-target effects in non-viral siRNA delivery. *Biomaterials, 32*(9), 2388-2398.

Moghimi, S. M., Symonds, P., Murray, J. C., Hunter, A. C., Debska, G., & Szewczyk, A. (2005). A two-stage poly (ethylenimine)-mediated cytotoxicity: implications for gene transfer/therapy. *Mol. Ther., 11*(6), 990-995.

Mukherjee, S. P., Lyng, F. M., Garcia, A., Davoren, M., & Byrne, H. J. (2010). Mechanistic studies of in vitro cytotoxicity of poly (amidoamine) dendrimers in mammalian cells. *Toxicol. Appl. Pharmacol., 248*(3), 259-268.

O'Mahony, A. M., Godinho, B. M. D. C., Cryan, J. F., & O'Driscoll, C. M. (2013a). Non-viral nanosystems for gene and siRNA delivery to the central nervous system: formulating the solution. *J. Pharm. Sci., 102*(10), 3469-3484.

O'Mahony, A. M., Godinho, B. M. D. C., Ogier, J., Devocelle, M., Darcy, R., Cryan, J. F., & O'Driscoll, C. M. (2012). Click-modified cyclodextrins as nonviral vectors for neuronal siRNA delivery. *ACS Chem. Neurosci., 3*(10), 744-752.

O'Mahony, A. M., Ogier, J., Darcy, R., Cryan, J. F., & O'Driscoll, C. M. (2013b). Cationic and PEGylated amphiphilic cyclodextrins: co-formulation opportunities for neuronal siRNA delivery. *PLoS One, 8*(6), e66413.

Omidi, Y., Hollins, A. J., Drayton, R. M., & Akhtar, S. (2005). Polypropylenimine dendrimer-induced gene expression changes: the effect of complexation with DNA, dendrimer generation and cell type. *J. Drug Target., 13*(7), 431-443.

Ramsay, R. G., Ciznadija, D., Vanevski, M., & Mantamadiotis, T. (2003). Transcriptional regulation of cyclo-oxygenase expression: three pillars of control. *Int. J. Immunopathol. Pharmacol., 16*(2 Suppl), 59-67.

Rawlinson, L.-A. B., O'Brien, P. J., & Brayden, D. J. (2010). High content analysis of cytotoxic effects of pDMAEMA on human intestinal epithelial and monocyte cultures. *J. Control. Release, 146*(1), 84-92.

Rejman, J., Oberle, V., Zuhorn, I., & Hoekstra, D. (2004). Size-dependent internalization of particles via the pathways of clathrin-and caveolae-mediated endocytosis. *Biochem. J., 377*, 159-169.

Rigamonti, D., Bauer, J. H., De-Fraja, C., Conti, L., Sipione, S., Sciorati, C., Clementi, E., Hackam, A., Hayden, M. R., Li, Y., Cooper, J. K., Ross, C. A., Govoni, S., Vincenz, C., & Cattaneo, E. (2000). Wild-Type Huntingtin Protects from Apoptosis Upstream of Caspase-3. *J. Neurosci., 20*(10), 3705-3713.

Sah, D. W. Y. (2006). Therapeutic potential of RNA interference for neurological disorders. *Life Sci., 79*(19), 1773-1780.

Sakurai, F., Terada, T., Yasuda, K., Yamashita, F., Takakura, Y., & Hashida, M. (2002). The role of tissue macrophages in the induction of proinflammatory cytokine production following intravenous injection of lipoplexes. *Gene Ther., 9*(16), 1120-1126.

Tanaka, T., Legat, A., Adam, E., Steuve, J., Gatot, J.-S., Vandenbranden, M., Ulianov, L., Lonez, C., Ruysschaert, J.-M., Muraille, E., Tuynder, M., Goldman, M., & Jacquet, A. (2008). DiC14-amidine cationic liposomes stimulate myeloid dendritic cells through Toll-like receptor 4. *Eur. J. Immunol., 38*(5), 1351-1357.

Thomas, C. E., Ehrhardt, A., & Kay, M. A. (2003). Progress and problems with the use of viral vectors for gene therapy. *Nat Rev Genet, 4*(5), 346-358.

Tönges, L., Lingor, P., Egle, R., Dietz, G. P. H., Fahr, A., & Bahr, M. (2006). Stearylated octaarginine and artificial virus-like particles for transfection of siRNA into primary rat neurons. *RNA, 12*(7), 1431-1438.

Uchida, E., Mizuguchi, H., Ishii-Watabe, A., & Hayakawa, T. (2002). Comparison of the efficiency and safety of non-viral vector-mediated gene transfer into a wide range of human cells. *Biol. Pharm. Bull., 25*(7), 891-897.

Van Cruchten, S., & Van Den Broeck, W. (2002). Morphological and biochemical aspects of apoptosis, oncosis and necrosis. *Anat. Histol. Embryol., 31*(4), 214-223.

Vangasseri, D. P., Cui, Z., Chen, W., Hokey, D. A., Falo, L. D., & Huang, L. (2006). Immunostimulation of dendritic cells by cationic liposomes. *Mol. Membr. Biol., 23*(5), 385-395.

Wang, Y. L., Liu, W., Wada, E., Murata, M., Wada, K., & Kanazawa, I. (2005). Clinico-pathological rescue of a model mouse of Huntington's disease by siRNA. *Neurosci. Res., 53*(3), 241-249.

Yamano, S., Dai, J., & Moursi, A. M. (2010). Comparison of transfection efficiency of nonviral gene transfer reagents. *Mol. Biotechnol., 46*(3), 287-300.